

## **General Disclaimer**

### **One or more of the Following Statements may affect this Document**

- This document has been reproduced from the best copy furnished by the organizational source. It is being released in the interest of making available as much information as possible.
- This document may contain data, which exceeds the sheet parameters. It was furnished in this condition by the organizational source and is the best copy available.
- This document may contain tone-on-tone or color graphs, charts and/or pictures, which have been reproduced in black and white.
- This document is paginated as submitted by the original source.
- Portions of this document are not fully legible due to the historical nature of some of the material. However, it is the best reproduction available from the original submission.

RECEIVED BY  
NASA STI FACILITY  
DATE: 6-19-78  
DCAF NO. 003662

*Not on RECON  
6-24-78*

PROCESSED BY  
 NASA STI FACILITY  
 ESA - SDS  AIAA



# UNIVERSITY OF SOUTHAMPTON

department of  
aeronautics  
and astronautics

Self Streamlining Wind Tunnel -  
Further Low Speed Testing and Final  
Design Studies for the Transonic  
Facility.

Semi-annual progress report to  
December 1977.

(NASA-CR-157111) SELF STREAMLINING WIND  
TUNNEL: FURTHER LOW SPEED TESTING AND FINAL  
DESIGN STUDIES FOR THE TRANSONIC FACILITY  
Semiannual Progress Report, period ending  
Dec. 1977 (Southampton Univ.) 37 p HC

N78-27141

Unclas  
G3/09 23559

SELF STREAMLINING WIND TUNNEL -  
FURTHER LOW SPEED TESTING AND FINAL  
DESIGN STUDIES FOR THE TRANSONIC  
FACILITY

by

S. W. D. Wolf

Department of Aeronautics & Astronautics,  
The University,  
Southampton, U.K.

This is a semi-annual Report, for the period to December 1977, on work undertaken on NASA Grant NSG-7172 entitled "The Self Streamlining of the Test Section of a Transonic Wind Tunnel". The Principle Investigator is Dr. M. J. Goodyer.

## C O N T E N T S

1. Introduction
2. Low Speed Self Streamlining Wind Tunnel Research (continued)
3. Comparison of Streamline and Elastic Structure Contours
4. Transonic Self-Streamlining Wind Tunnel Control System
5. Conclusions

List of Symbols

List of References

Figures

1. INTRODUCTION

Work has continued with the low speed Self Streamlining Wind Tunnel (SSWT) using the MACA 0012-64 airfoil in an effort to explain the discrepancies between the NASA Langley Low Turbulence Pressure Tunnel (LTPT) and SSWT results obtained with the airfoil stalled. Conventional wind tunnel corrections have been applied to straight wall SSWT airfoil data, to illustrate the inadequacy of standard correction techniques in circumstances of high blockage. Also one SSWT test has been re-run at different air speeds to investigate the effects of such changes (perhaps through changes in Reynold's number and freestream turbulence levels) on airfoil data and wall contours.

Mechanical design analyses for the Transonic Self-Streamlining Wind Tunnel (TSWT) have been completed by the application of theoretical airfoil flow field data to the elastic beam and streamline analysis.<sup>1</sup>

The control system for the transonic facility, which will eventually allow on-line computer operation of the wind tunnel, is outlined.

## 2. LOW SPEED SELF STREAMLINING WIND TUNNEL RESEARCH (Continued)

No modifications have been incorporated into the SSWT since the preceding progress report<sup>1</sup>, and work with the wind tunnel has centered on isolating the cause of discrepancies in airfoil data when the NACA 0012-64 airfoil is stalled at  $\alpha > + 8^{\circ}$ . In this regime, the suction surface of the airfoil supports large regions of separated flow, which are susceptible to any secondary flow effects present in the wind tunnel.

Variation of wind tunnel airspeed affects both the freestream turbulence level and the chord Reynolds number  $R_c$ . The airfoil model used in SSWT has always had transition strips attached near to its leading edge, but when the wing is stalled the effectiveness of these strips is probably reduced, particularly at low values of Reynolds number. Four SSWT runs were performed over a range of  $R_c$  from 170,000 to 370,000. Throughout these tests the flexible walls were set to the same contours as determined for Run 180 and were not re-streamlined to account for the effects, if any, of change in Reynolds number. In these tests there were transition strips applied to the airfoil but no wing fences<sup>1</sup>, and  $\alpha$  was constant at  $12.1^{\circ}$ . Figure 2.1. illustrates how both  $C_N$  and  $C_c$  varied with  $R_c$ .

The new SSWT data indicates a gradual increase of  $C_N$  with  $R_c$  but the converse for  $C_c$ , although the overall variation in values is less than 10% over the  $R_c$  range. The LTPT data is also shown, with no variation apparent in either  $C_N$  or  $C_c$ , over the narrow range of  $R_c$ . Notice that a very large effect would be required to bring SSWT data into agreement with LTPT results, namely a 25% reduction in  $C_N$  and a 30% increase in  $C_c$ .

With SSWT apparently in an identical configuration as for run 180, it is interesting to see that the re-run (run 224) has produced different results at the same value of  $R_c$ , namely a .0324 reduction in  $C_N$  and a

.0116 increase in  $C_c$ . It was found from examination of the differences between real and imaginary pressure coefficients along the flexible walls that they were not well streamlined during any of the new tests from which the data presented on figure 2.1. was obtained. A measure of pressure imbalance along a wall is  $E_{C_p}$ , the average pressure coefficient error for each wall. The errors for the new tests are shown on figure 2.2., all lying above the error which is presently regarded as acceptable in SSWT,  $E_{C_p} = 0.015$ .

Possible reasons for data disparity include the re-gritting of the leading edges which had taken place since run 180, and an error in setting angle of attack. A re-streamlining was therefore decided upon (run 228) at the approximate Reynolds number of the LTPT tests and at  $\alpha = 12.1^\circ$ .

Figure 2.3. shows the changes in airfoil pressure distributions between runs 180 and 228, both runs being at the same Reynolds numbers and angle of attack, and both with the walls streamlined. A problem of test repeatability is revealed which will require attention.

Even though most data points shown on figures 2.1. were taken with walls inadequately streamlined, the weak variations of force coefficients with Reynolds number, coupled with the small changes in coefficients with the one re-streamlining that was carried out, indicate that data discrepancies between SSWP and LTPT at high angles of attack were not likely to be due to small differences in Reynolds number. It is proposed to explore the possibility that some consistent angle of attack errors exist in SSWT.

Straight wall SSWT  $C_N$  and  $C_c$  data has been converted to  $C_L$  ( $C_N$  and  $C_c$  data is already reported.<sup>1)</sup> The  $C_L$  data was corrected by the Goldstein method<sup>5</sup> for low speed wind tunnel interference and viscous effects. In addition there was a blockage correction made to the  $C_L$  data for values of  $\alpha > +9^\circ$ , where the separated wake of the stalled airfoil resembles

the wake of a bluff body, as postulated by Maskell<sup>5</sup>. Despite the fact that standard wind tunnel corrections are made by use of small perturbation theory where  $c/h$  is assumed to be small, but in fact in these tests the ratio was high at 0.9, useful corrections have been achieved. These are illustrated by the complete available range of airfoil  $C_L$  data shown in Figures 2.4. In the unstalled regime, the corrected SSWT data compare favourably with the LTPT values for which standard corrections are insignificant. This data is conveniently summarised by fitting straight lines through the data over the range  $-6^\circ \leq \alpha \leq +8^\circ$ , using a least squares method. The slopes and intercepts of these line fits are as follows:-

Data source	$\delta C_L / \delta \alpha$ per degree	Zero Intercept $C_L$
LTPT	0.0847	0.0095
Streamlined Wall SSWT	0.0824	- 0.01945
Straight Wall SSWT - Corrected	0.088	- 0.0077
Uncorrected	0.098	- 0.0086

The lift curve slope ratios

$$\frac{\text{SSWT, straight wall, corrected}}{\text{LTPT}}$$

and

$$\frac{\text{SSWT, streamlined walls}}{\text{LTPT}}$$

respectively 1.039 and 0.973.

It is interesting to see that the straight wall SSWT corrected  $C_L$  values tend to be larger than the corresponding LTPT values, while the streamlined wall SSWT data tends to be below LTPT. This may point to some form of over correction of wind tunnel interference in the streamlined wall SSWT tests.

The stalled regime is more confused, with the likelihood of secondary flow effects. The straight walled SSWT uncorrected  $C_L$  data does not indicate any airfoil stall. Figure 2.5. is an example of airfoil pressure distributions at  $\alpha = 11^\circ$  (this is new data) with straight and streamlined walls. Note the large suction loop supported by the airfoil before streamlining.

An example of the effectiveness of streamlining in comparison with the alternative of data correction at high  $\alpha$  is the data at  $\alpha = 12^\circ$ . Assuming the LTPT data to be correct, applying conventional corrections to straight wall SSWT data reduces the  $C_L$  error from 128% to 44%, whereas wall streamlining has reduced the error from 128% to 28%.

### 3. COMPARISON OF STREAMLINE AND ELASTIC STRUCTURE CONTOURS

Theoretical data on streamlines around an unstalled NACA 0012-64 section at  $\alpha = +8^\circ$ , in a free stream at Mach 0.8, has become available. This has been applied to the elastic beam and streamline analysis described in the preceding progress report.<sup>1</sup>

In this analysis the elastic beam, representing the flexible wall, is constrained to pass through a finite number of points along a streamline, the points representing jacks. Between any two points the contours of the streamline and the elastic beam differ from each other. It is assumed that this difference increases from zero at a jack, to a maximum roughly mid-way between jacking points. The beam was constrained to pass through a group of six equally spaced points along a streamline. The difference or error between the elastic beam and streamline at the center of this group,  $E_w$ , was examined, as affected by jack spacing and changes in the position of the beam center along the streamline. The results are shown in figure 3.1. for streamlines spaced half a chord above and below the airfoil and for two jack spacings.

$E_w$  reaches a maximum with the beam center approximately over the airfoil quarter-chord point on the top wall and under the airfoil leading edge on the bottom wall. The effect of jack spacing on the position of these maxima is small. Notice that the behaviour of  $E_w$  is oscillatory, damping out to almost zero as the beam centre moves out of close proximity with the model. The wavelength of these oscillations is approximately twice the jack spacing.

This evidence suggests that  $E_w$  can be minimised by positioning a jack over the airfoil quarter-chord point on the top wall and under the leading edge on the bottom wall. This would have the effect of perhaps eliminating the maximum value of  $E_w$ , ( $E_{wm}$ ), and the secondary peak values, if the jacking system incorporates equal jack spacing in the vicinity of the model.

A wider ranging survey was carried out, the values of maximum error  $E_{wm}$  assumed to occur when the beam mid-point coincided with the airfoil quarter chord point on the top wall and the leading edge on the bottom wall. The data is shown in figure 3.2. for variables including three test section depths ( $h/c = 0.5, 1, 2$ ) and jack spacings up to 1.8 chords. As could be expected, the shallower the test section, the more rapid is the rise in value of  $E_{wm}$  with increasing jack spacing. Also prominent are the differences in behaviour between upper and lower walls. The double curvature of the lower wall necessitates closer jack spacing in the neighbourhood of the model. With a test section height to model chord ratio ( $h/c$ ) of 1, the wall setting tolerances adopted in the design of the transonic SSWT can be met with a jack spacing of 0.56 chord on the upper wall, but only 0.34 chord on the lower wall. When a large chord model (say 15 cm) is combined with the minimum depth of test section available on the transonic test section (7.6 cm), giving  $h/c \approx 0.5$ , the data on figure 3.2b indicates that it may prove necessary to position a jack under the airfoil leading edge. This is because with poorly located jacks, the jack spacing of 2.54 cm will result in a spacing: chord ratio of 0.166 and a ratio  $E_{wm}/c \approx -0.005$  giving a wall error of .75 mm (0.03 inches) which is regarded as unacceptably high.

Further work has involved an examination of the effect of lift on  $E_w$  in the vicinity of the model, this time using potential flow streamlines round a lifting cylinder. Figure 3.3. shows the findings of this work for  $C_L$  in the range  $\pm 4$ . At larger jack spacings, say above about 75% of the test section height, change in  $C_L$  has a relatively small effect on the position accuracy of wall adjacent to the suction surface, but there is a significant effect associated with the other wall. This is again a result of the double curvature in the wall adjacent to the pressure surface. For the smaller jack spacings that are primarily of interest (below .5 test

section height), the wall adjacent to the pressure surface of the model is seen to contain the largest errors. For example, with a ratio of  $E_w$  to cylinder diameter of .0025 (corresponding to the chosen error limit) and with  $C_L = 4$ , the upper wall jack spacing can be up to .38h, while only a spacing of .27h is permissible on the lower wall in the vicinity of the model.

It should be noted that the errors shown on figure 3.3. probably represent the largest likely to occur, because of an unfavourable positioning of jacks relative to the model. If jacks had been positioned above and below the cylinder axis, the errors may be much reduced.

This particular example of a lifting cylinder would produce a blockage of 33% and its behaviour could therefore be taken as indicative of that associated with an airfoil at high angles of attack.

#### 4. TRANSONIC TEST SECTION CONTROL SYSTEM

The function of the on-line computer control system for the Transonic Self-Streamlining Wind Tunnel (TSWT) is:-

- a) To streamline the flexible walls.
- b) To acquire test data from the model.

The basic operation has already been defined<sup>4</sup>, and the system can be divided into hardware (at the wind tunnel site) and software (in the computer memory).

The control system's software is outlined by a flow diagram in figure 4.1. The box labelled 'Compute', refers to the running of the wall analysis program<sup>1</sup>, which determines the next pair of wall contours. Although already in use with the low speed SSWT, this program will require modification for application to transonic flows. Also to be added to this program is a control segment, which will include a software interface between computer and wind tunnel.

The control system's hardware is shown schematically in figure 4.2. The diagram is sub-divided into three sections, comprising items at the computer, items at the wind tunnel, and the control system's functions. There are four actions required: screw jack movement, wall jack position measurement, pressure port scan and the air pressure measurements on the tunnel walls and model. Basically the system comprises two feedback loops, one to control the wall contours and another to step the four scanivalves (which are chained together) round each pressure port. Data from the pressure transducers is fed to the computer by a semi-independent route.

A PDM-70-CB Programmable Data Mover (PDM) provides the necessary interface between the PDP 11 computer and the wind tunnel facility. While its prime function is to move data, the PDM also incorporates several peripheral items concerned with analogue to digital signal conversion and a serial information link with the computer. Information from the PDM to

the wind tunnel will be multiplexed.

To facilitate the controlled movement of the flexible walls, each of the forty screw jacks has its own motor drive unit, which stores direction information and supplies 3-phase power, with a 1.4 amp peak current, in the correct sequence to its associated stepper motor. The 3-phase supply is provided by a single pulse sequence generator at a fixed pulse rate (expected to be 200 pulses per sec) and in short bursts sufficient to move each jack a predetermined increment of movement. This 3-phase power signal is in fact split into two, each half driving a maximum of twenty jacks, therefore only half the stepper motors are powered at any one instant. The power supply provides a stabilised single phase 30 volt signal at 30 amps, and incorporates various protection devices and forced air cooling. It is run off the 50 cycle 240 volts mains. Figure 4.3. shows a circuit diagram of this equipment, together with those of the motor drive unit and the pulse sequence generator.

Other sub-systems are the scanivalve drive unit which performs motor drive and valve position sensing functions, and the various transducer bridges which provide analogue information on flexible wall positions and all wind tunnel pressures.

Control of the entire system will be via a VDU terminal, which has an entirely independent link with the computer. The VDU will also allow immediate display of reduced test data at the wind tunnel site.

Due to the complexity of the control system, several safety devices have been incorporated into both the hardware and the software. These are:-

1. Position measurement of each jack after every increment of movement to monitor the performance of the stepper motor-potentiometer pairs, and the power supply.
2. Power is only applied to the stepper motors in short bursts, and there is a time switch to eliminate any run-on which might occur,

for example, due to computer or control system failures.

3. Pressure port scans will include wind tunnel reference pressures at regular time intervals to check for Mach number variations.
4. Stops on the screw jacks to limit their movement.

Most items of the control system are ready, but some hardware, principally the multiplexers, is designed but as yet un-built. The interfacing between computer and wind tunnel currently provides the largest obstacle to completion of the on-line control system. However, it is planned that the transonic facility will be initially operated in a manual mode, similar to that presently employed with the low speed SSWT, but with much reduced streamlining times.

Ultimately, the TSWT will be operated in the following sequence (refer to figure 4.1):

1. The model is adjusted to the required attitude and all the electronics are switched on at the wind tunnel.
2. The command 'run' is typed on the VDU and sent to the computer.
3. All conditions at the wind tunnel (i.e. jack positions) are reset to known values in the computer's memory.
4. The command 'start' is given to the computer and the tunnel is activated.
5. The computer acquires all flexible wall static pressures.
6. New wall contours are computed.
7. The computer determines the size and direction of the movement required at each jack.
8. All jacks needing adjustment move one predetermined increment of movement, about .05 mm.
9. Pulse sequence generator reports 'move complete' to the computer.
10. Position data on each jack is acquired by the computer.
11. Steps 8 to 10 inclusive are repeated until the walls have the correct contours for that particular iteration.

12. Steps 5 to 11 inclusive are repeated until the walls are streamlined.
13. The computer acquires model data.
14. The computer reports 'finished with tunnel' and the wind tunnel is manually turned off.
15. The test data is analysed and the computed results displayed on the VDU for subsequent hard copy print-out.

The run time of the wind tunnel during this operation is expected to be as short as 2 minutes.

5. CONCLUSIONS

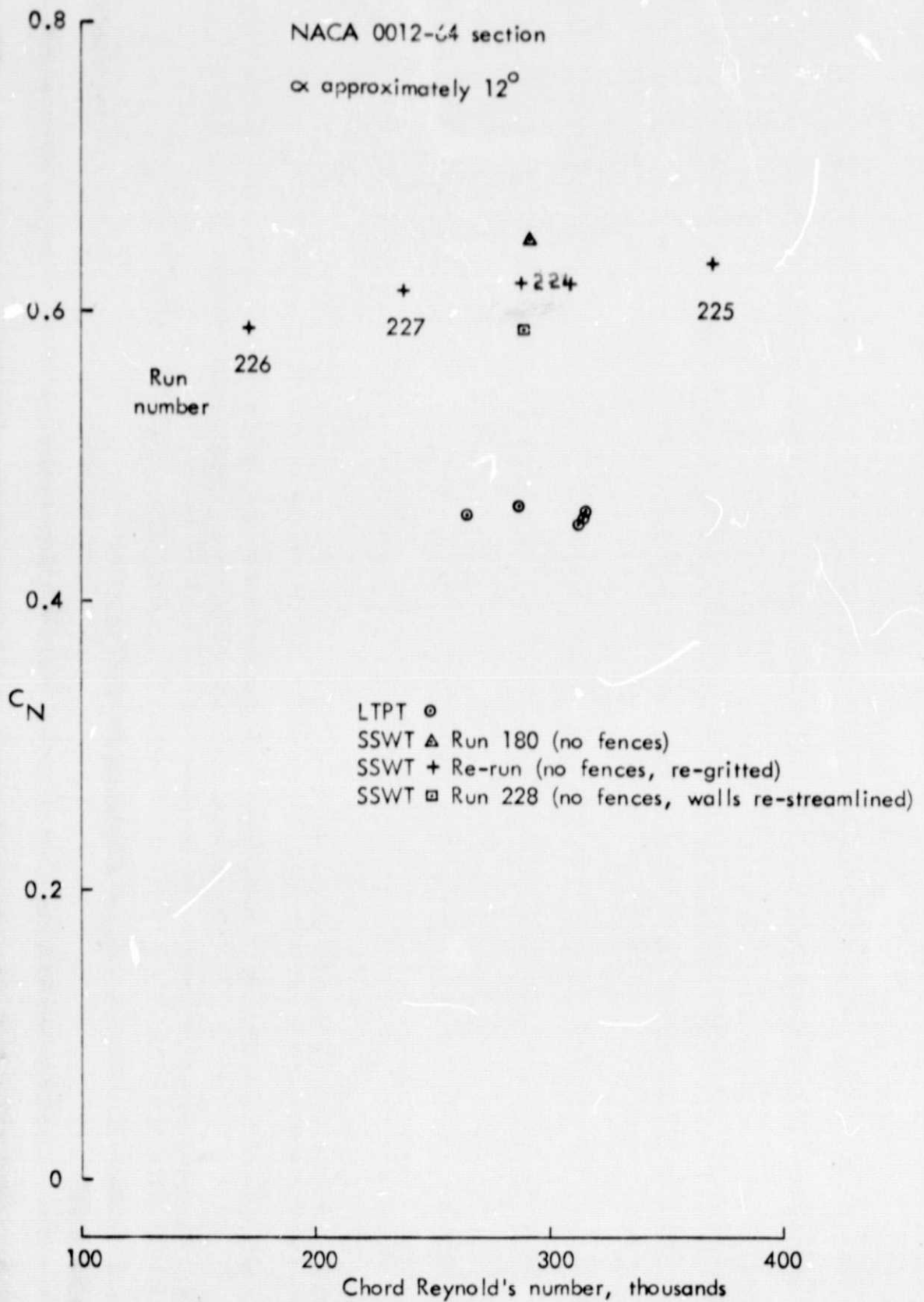
1. Causes of the discrepancies between SSWT and LTPT data on the NACA 0012-64 airfoil beyond stall remain unresolved.
2. The effect of Reynold's number on the streamlining of the SSWT is probably important.
3. The anticipated maximum wall position errors in the Transonic Self-Streamlining Wind Tunnel, introduced by wall mechanics, are within the limits set by prior aerodynamic considerations.
4. The detailed design of the TSWT control system for automatic wall streamlining and data acquisition, is finalised and the system is under development.

SYMBOLS

$c$	=	Wind chord
$R_C$	=	Chord Reynold's number
$\alpha$	=	angle of attack
$C_p$	=	pressure coefficient
$C_N$	=	normal force coefficient
$C_c$	=	chordwise force coefficient
$C_L$	=	lift coefficient
$h$	=	test section height
$E_w$	=	wall position error
$E_{wm}$	=	maximum wall position error
$X$	=	chordwise position downstream of airfoil $\frac{1}{2}$ chord point
$E_{cp}$	=	$C_p$ error averaged along a flexible wall
$x$	=	chordwise position on airfoil

## REFERENCES

1. S. W. D. Wolf and M. J. Goodyer 'Self streamlining Wind Tunnel - Low Speed Testing and Transonic Test Section Design'. NASA CR-145257.
2. M. Judd, S. W. D. Wolf and M. J. Goodyer 'Analytical Work in Support of the Design and Operation of Two Dimensional Self Streamlining Test Sections'. NASA CR-145019
3. M. J. Goodyer 'The Self Streamlining Wind Tunnel' NASA TMX-72699 August 1975.
4. M. Judd, M. J. Goodyer and S. W. D. Wolf 'Applications of the Computer for on-site Definition and Control of Wind Tunnel Shape for Minimum Boundary Interference'. AGARD Conference Proceedings No-210- Numerical Methods and Wind Tunnel Testing, June 1976.
5. H. C. Ganner, E. W. E. Rogers, W. A. E. Acum and E. C. Maskell 'Subsonic Wind Tunnel Wall Corrections' AGARDograph 109, October 1966.



ORIGINAL PAGE IS  
 OF POOR QUALITY

Figure 2.1a VARIATION OF AIRFOIL  $C_N$  WITH  $R_c$ .

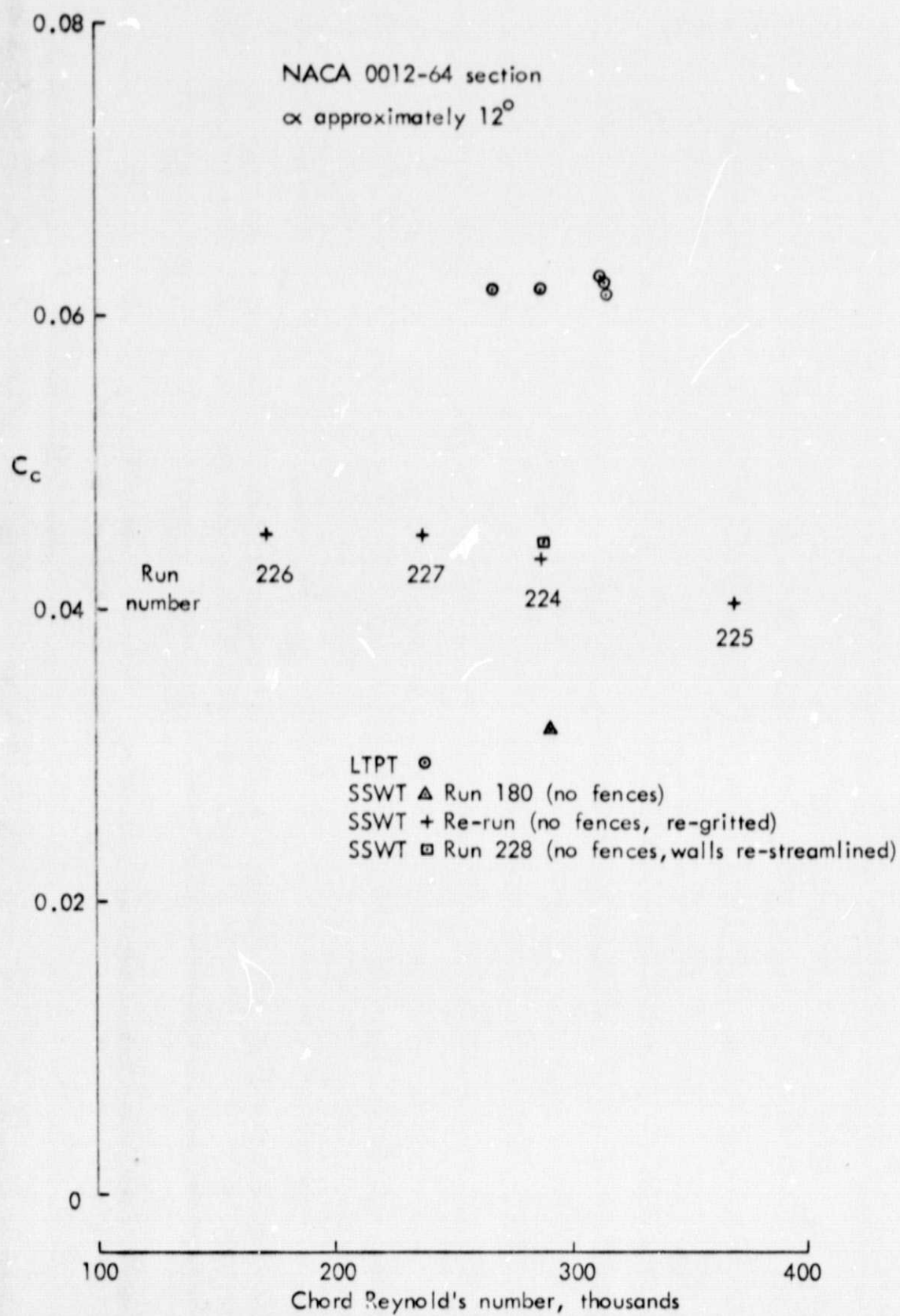


Figure 2.1b VARIATION OF AIRFOIL  $C_c$  WITH  $R_c$

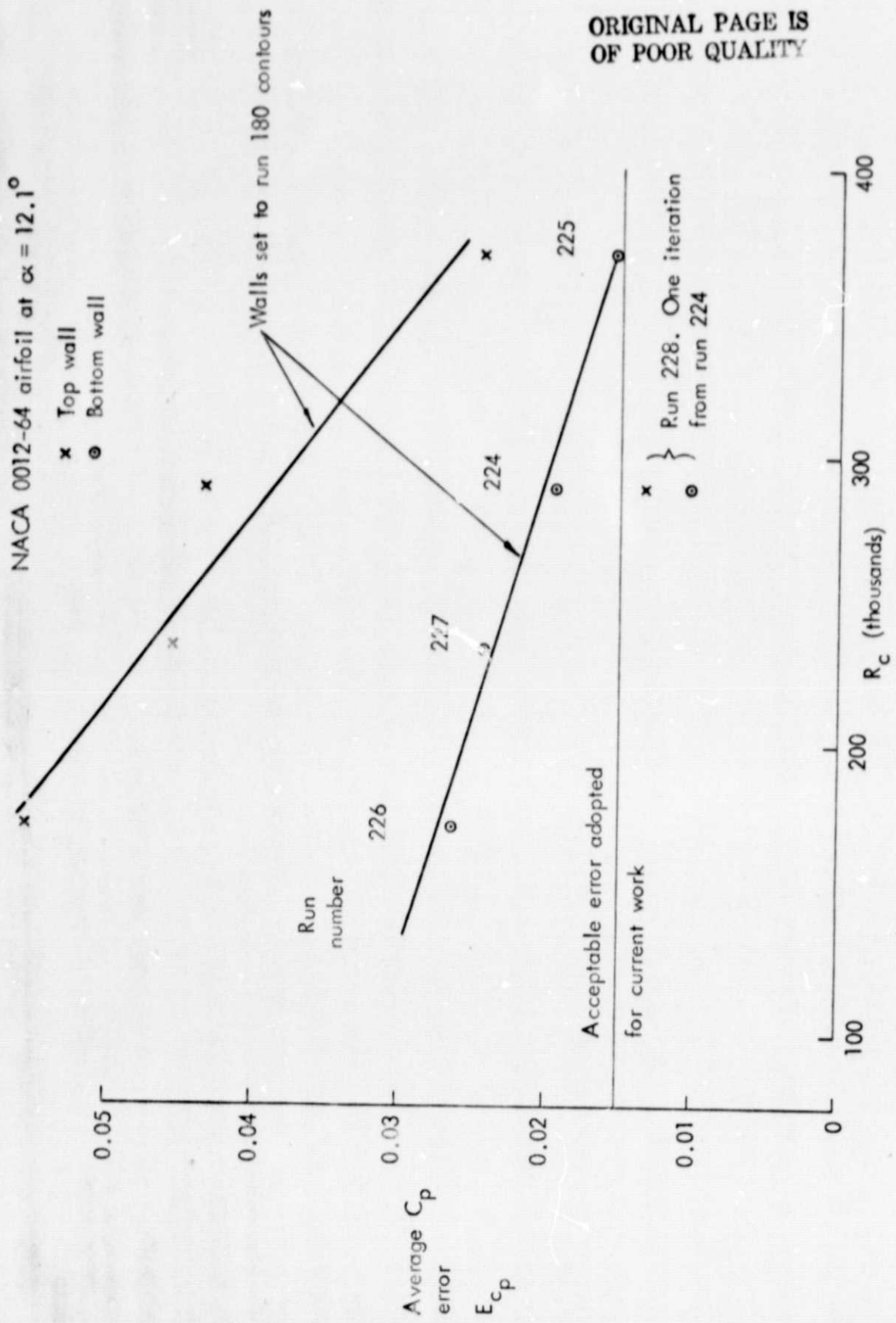


Figure 2.2 VARIATION OF FLEXIBLE WALL STREAMLINING WITH CHORD REYNOLD'S No.

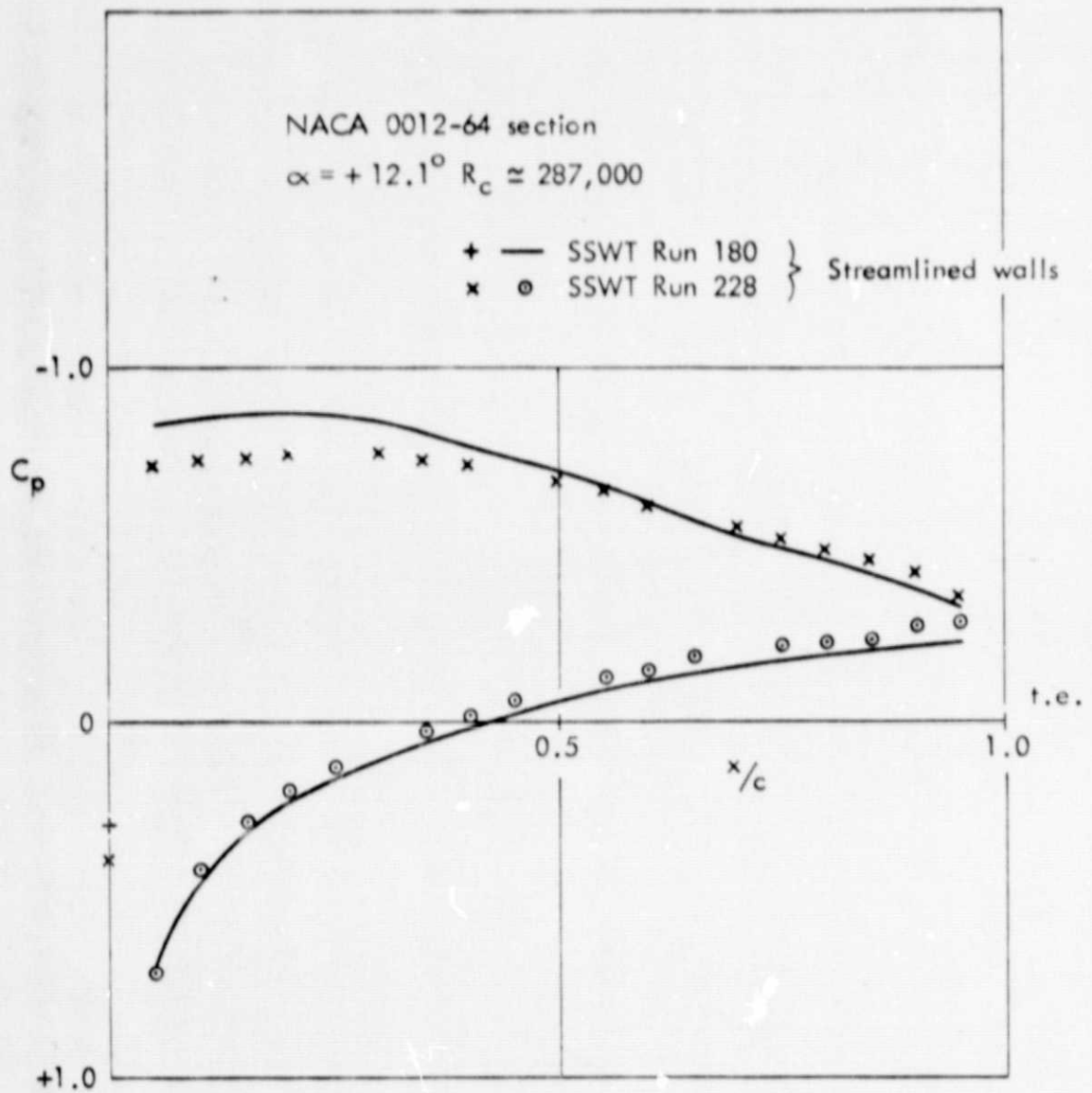


Figure 2.3 VARIATION IN AIRFOIL PRESSURE DISTRIBUTION FOR  $\alpha = 12.1^\circ$

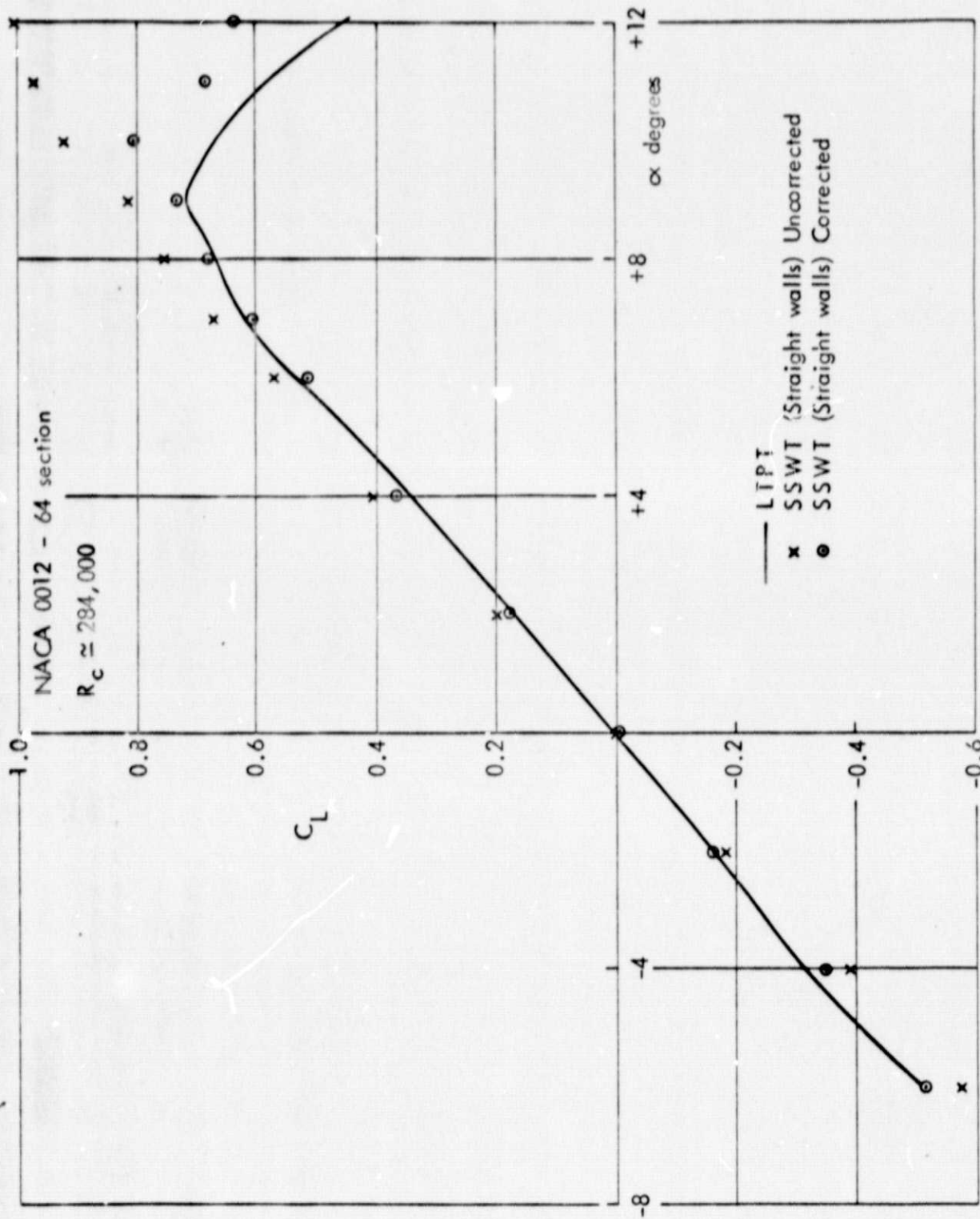


Figure 2.4a  $C_L$  DATA FROM THE STRAIGHT WALL SSWT AND LTPT.

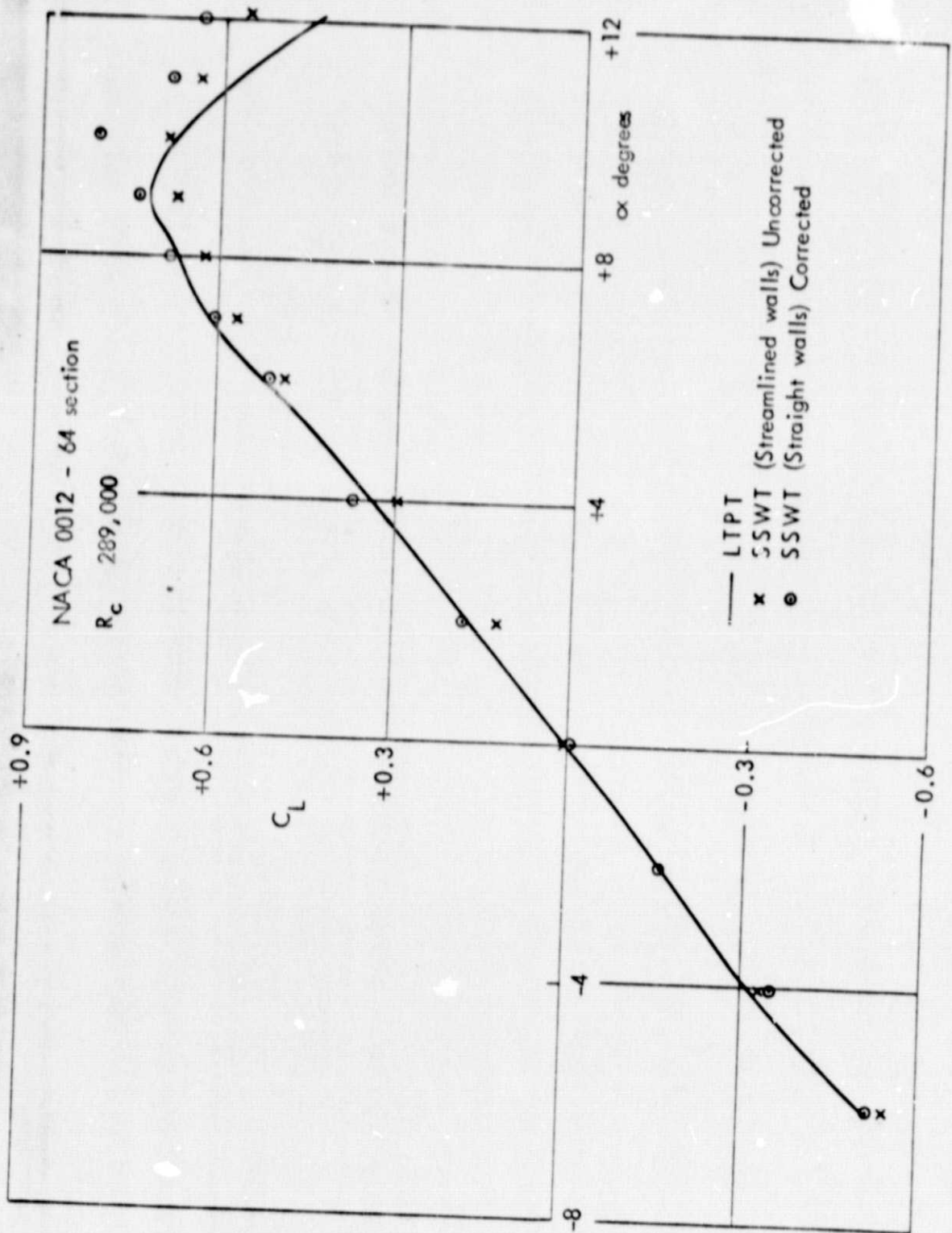


Figure 2.4b COMPARISON OF STREAMLINED WALL SSWT AND STRAIGHT WALL SSWT CORRECTED  $C_L$  DATA

NACA 0012-64 section  
 $\alpha = +11^\circ$   $R_c = 287,000$

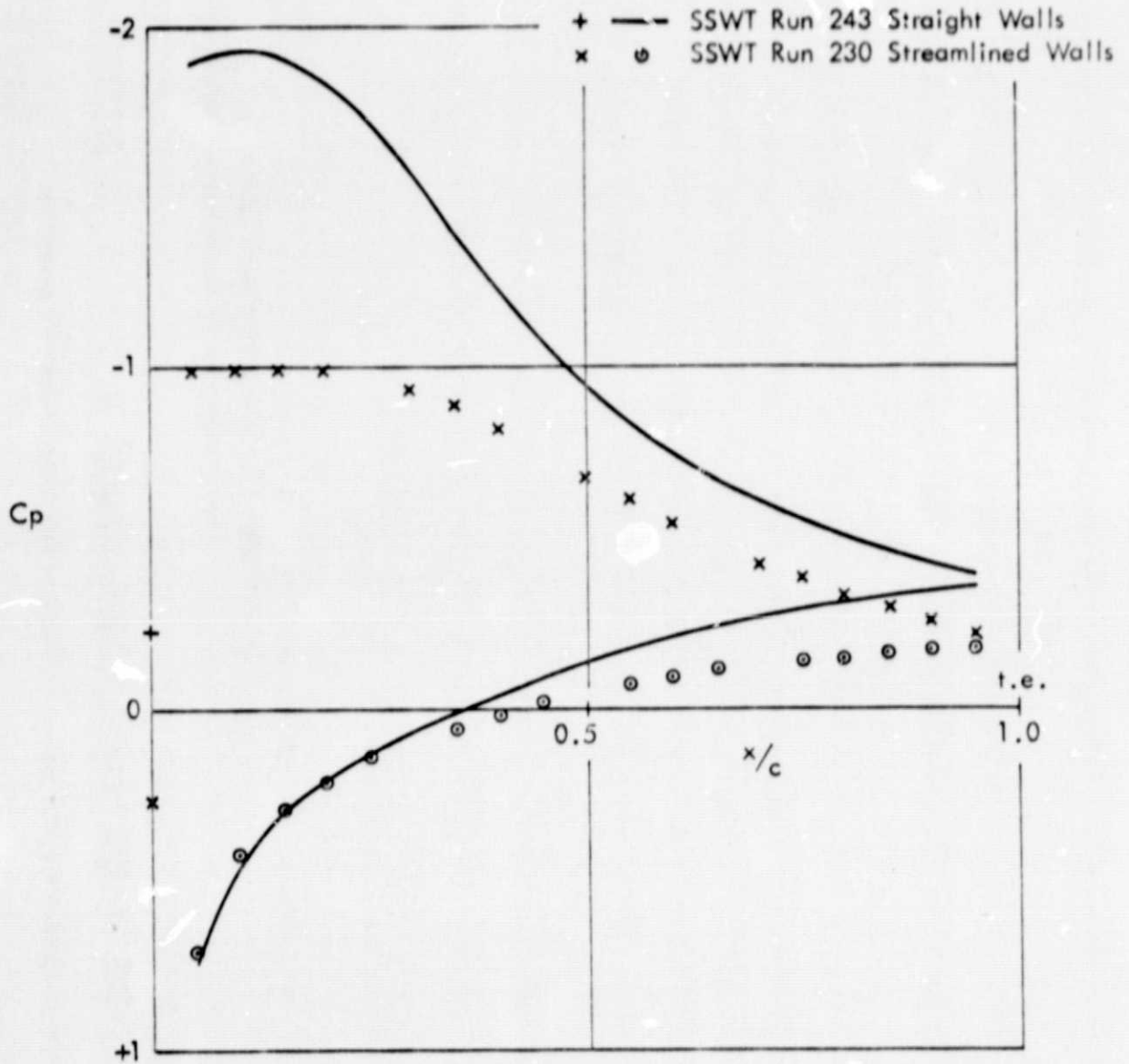


Figure 2.5 AIRFOIL PRESSURE DISTRIBUTION FOR  $\alpha = +11^\circ$  WITH SSWT FLEXIBLE WALLS SET STRAIGHT AND STREAMLINED

Comparison of upper wall theoretical streamlines and elastic structure contours.

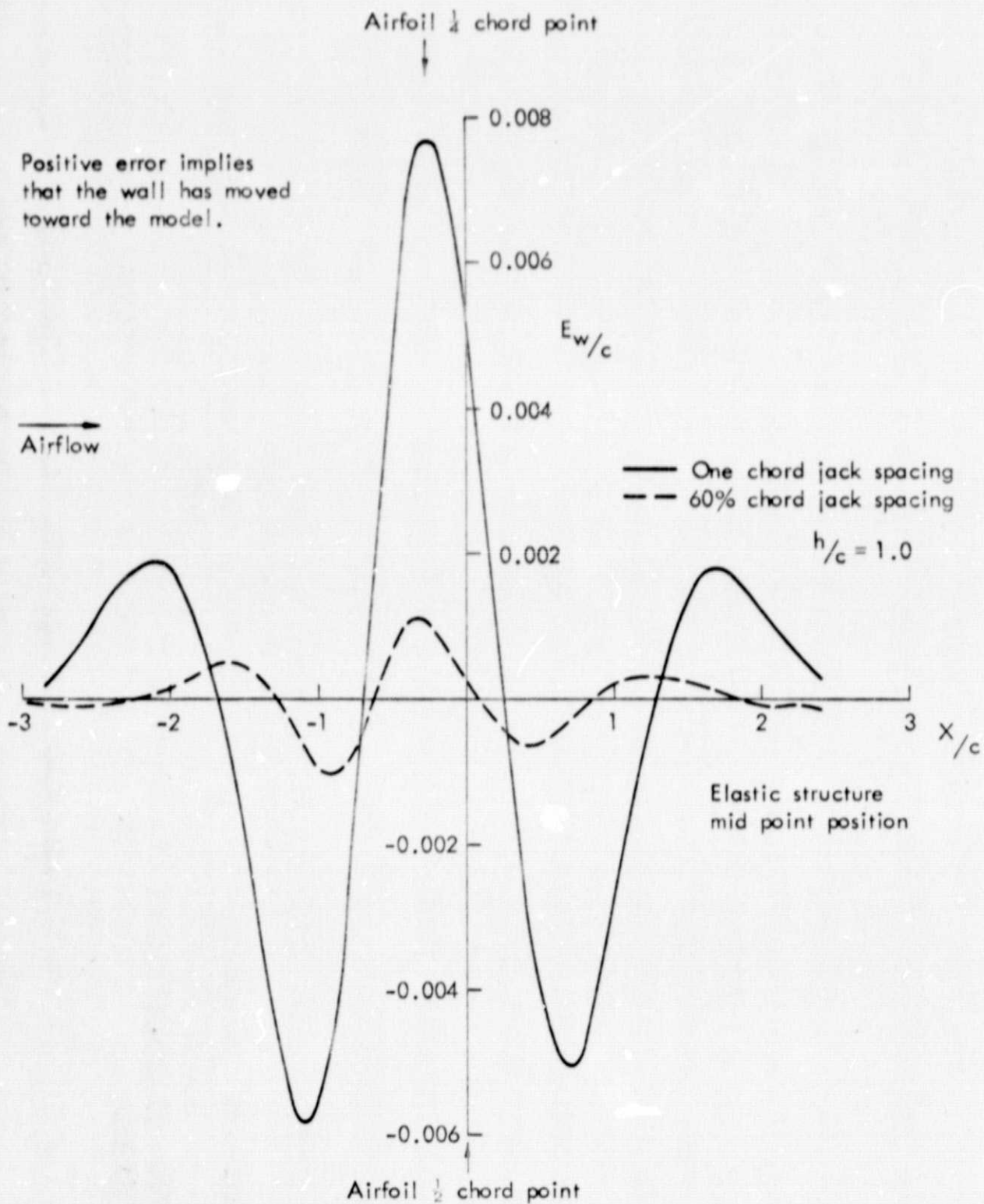


Figure 3.1a FLEXIBLE WALL POSITION ERROR ANALYSIS

Comparison of lower wall theoretical streamlines and elastic structure contours.

ORIGINAL PAGE IS  
OF POOR QUALITY

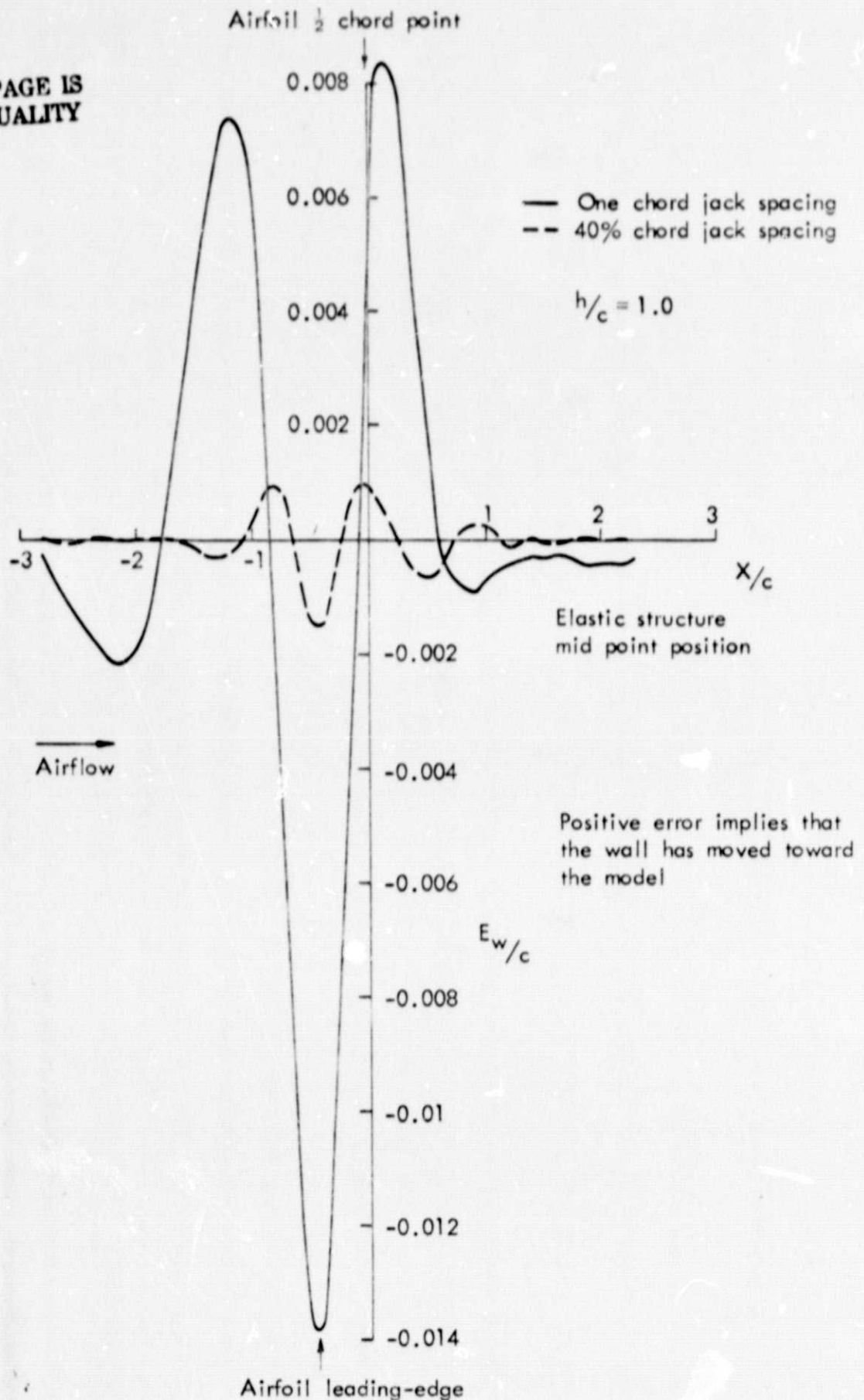


Figure 3.1b FLEXIBLE WALL POSITION ERROR ANALYSIS

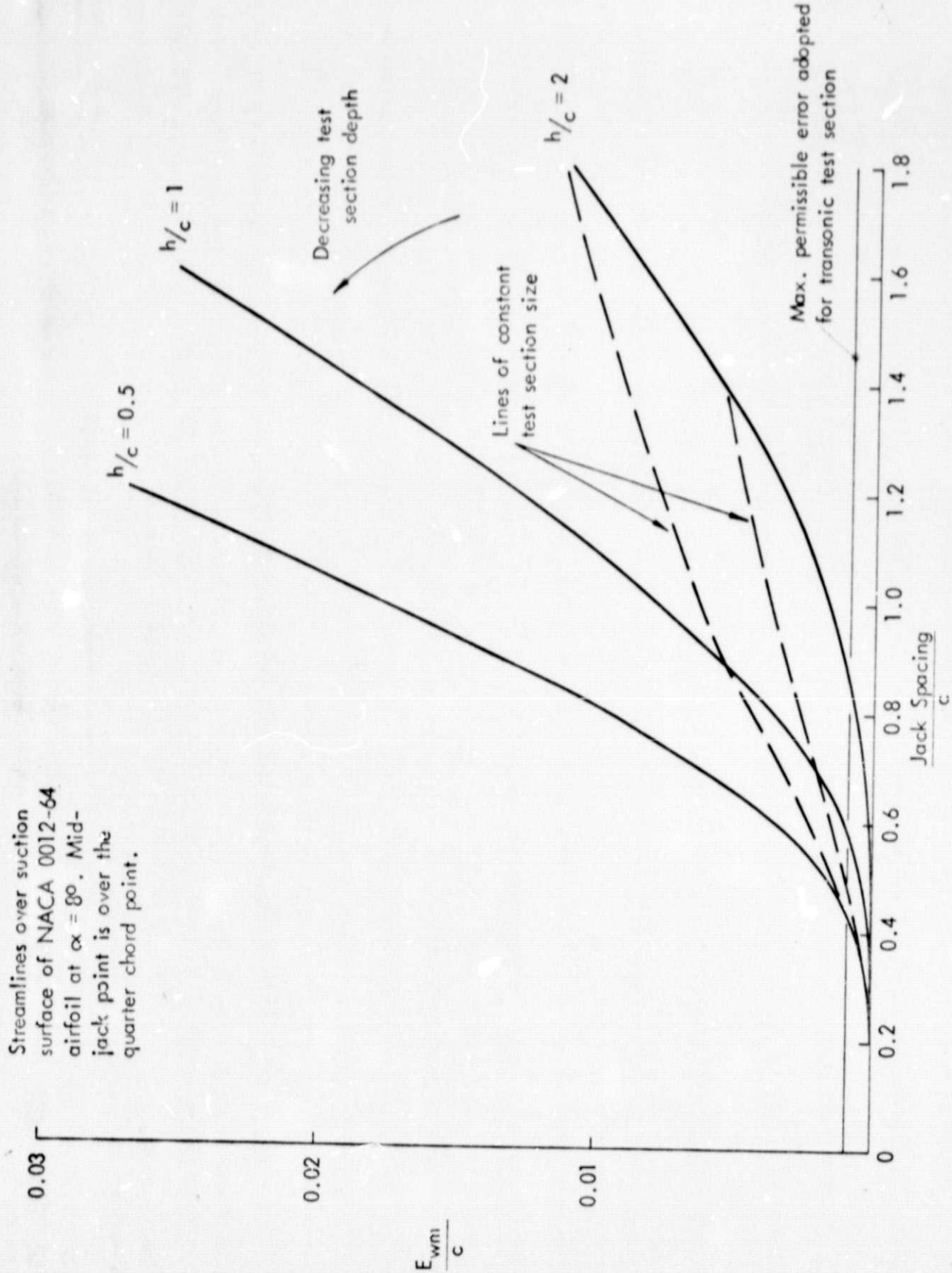


Figure 3.2a MAXIMUM ERRORS BETWEEN AIRFOIL STREAMLINES AND AN ELASTIC STRUCTURE.

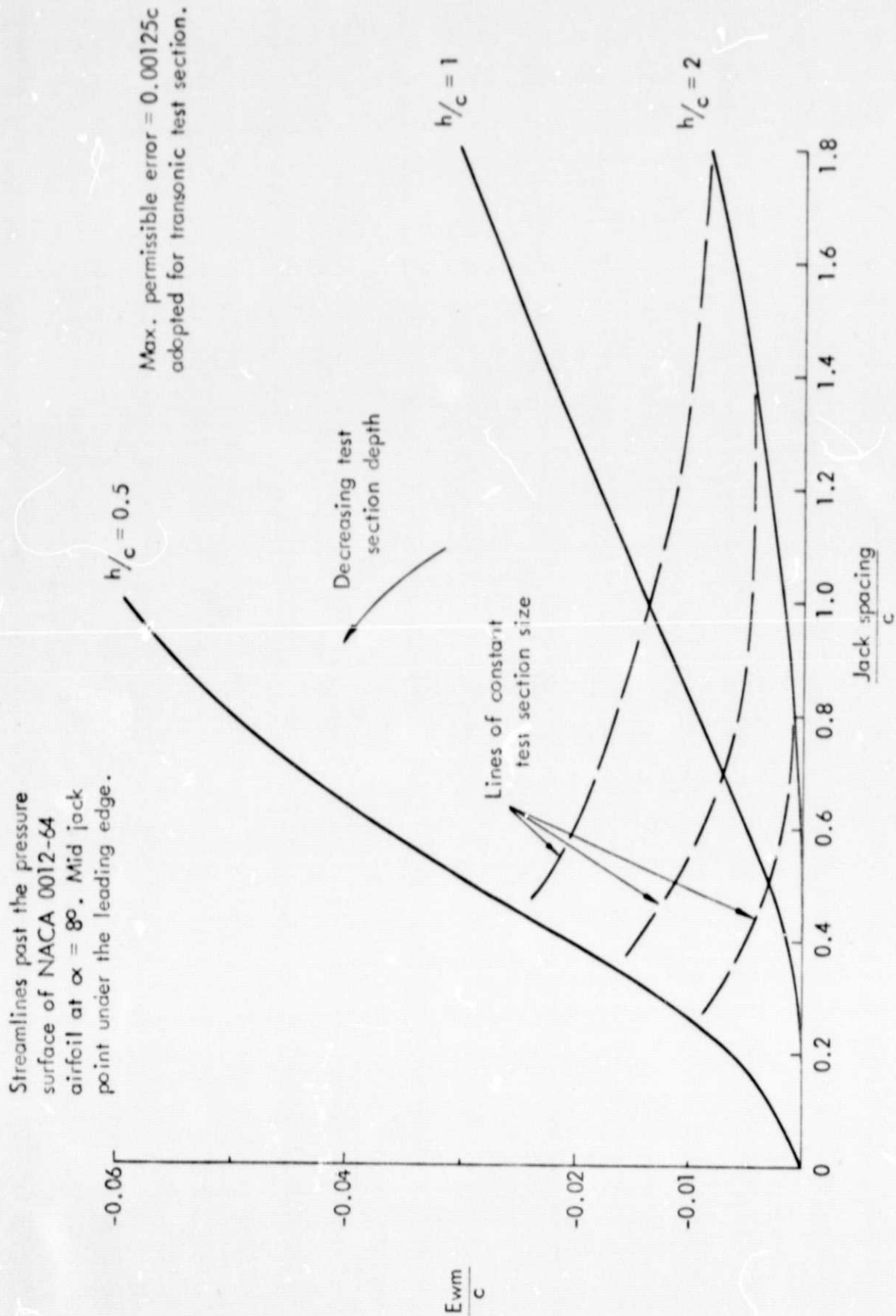


Figure 3.2b

MAXIMUM ERRORS BETWEEN AN AIRFOIL STREAMLINE AND AN ELASTIC STRUCTURE .

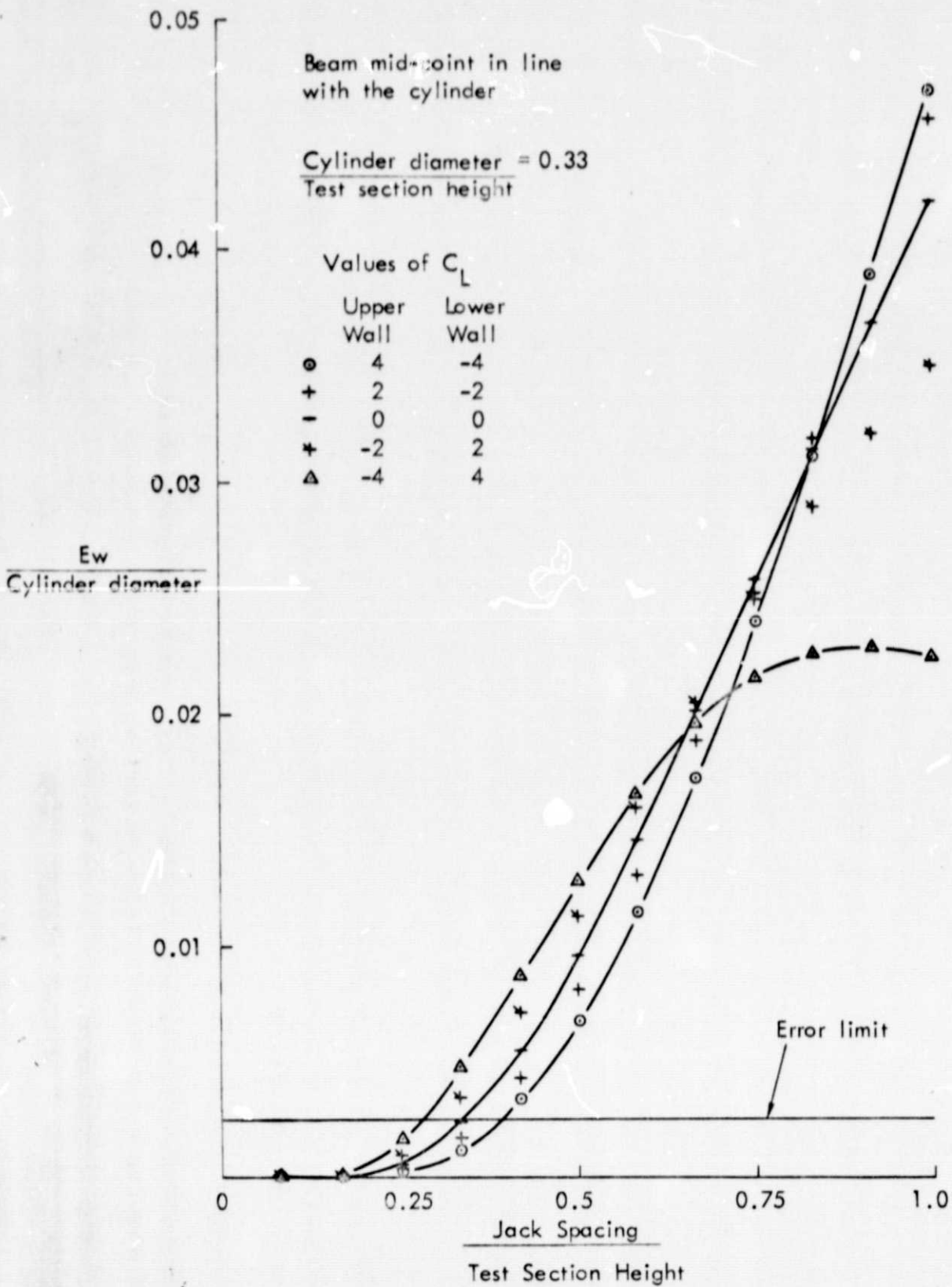


Figure 3.3 COMPARISON OF STREAMLINE AND ELASTIC STRUCTURE CONTOURS FOR POTENTIAL FLOW ROUND A LIFTING CYLINDER.

ORIGINAL PAGE IS  
OF POOR QUALITY

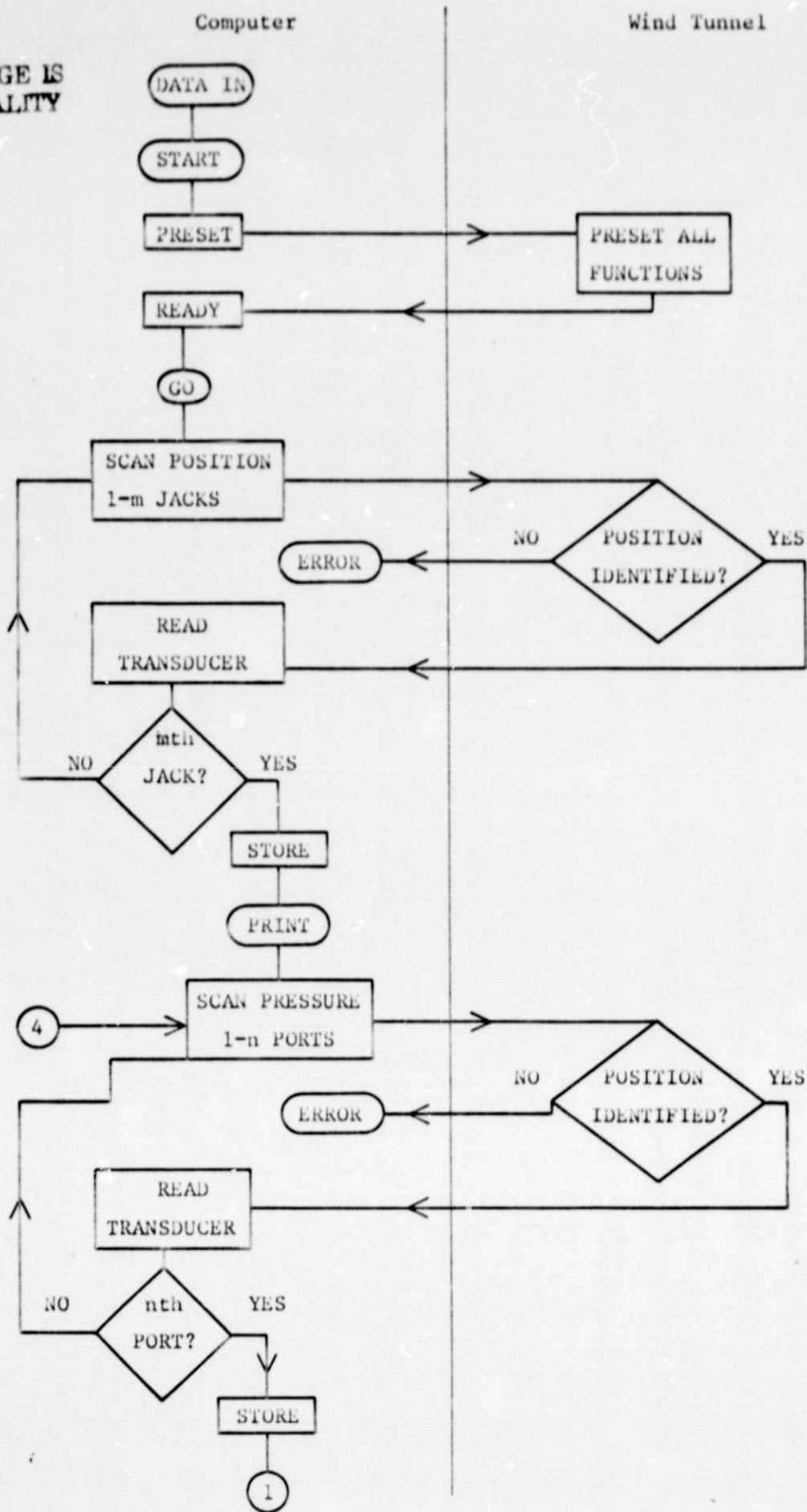


Figure 4.1a CONTROL SYSTEM FLOW DIAGRAM FOR TRANSONIC TEST SECTION

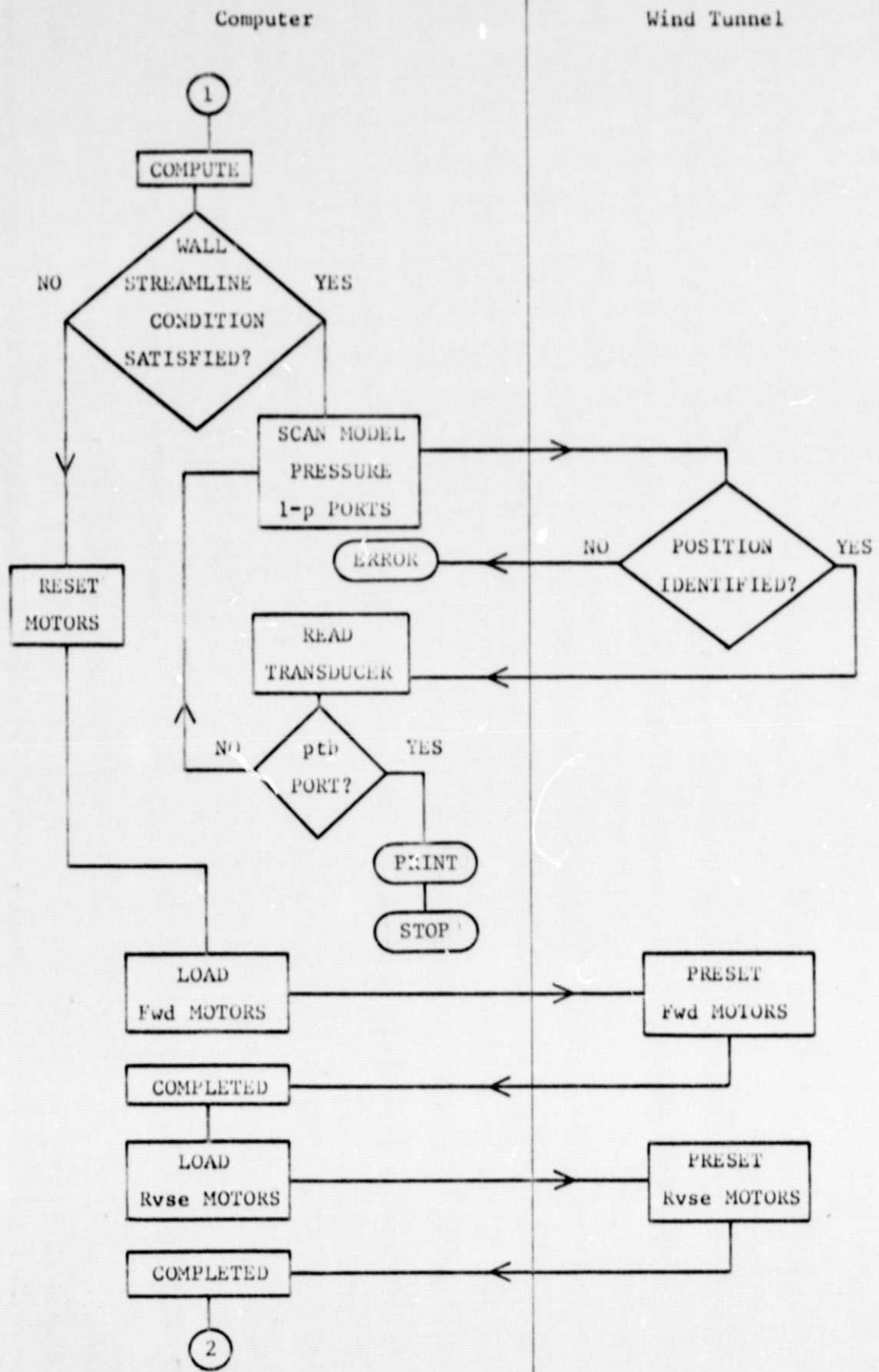


Figure 4.1b CONTROL SYSTEM FLOW DIAGRAM FOR TRANSONIC TEST SECTION (Continued)

ORIGINAL PAGE IS  
OF POOR QUALITY

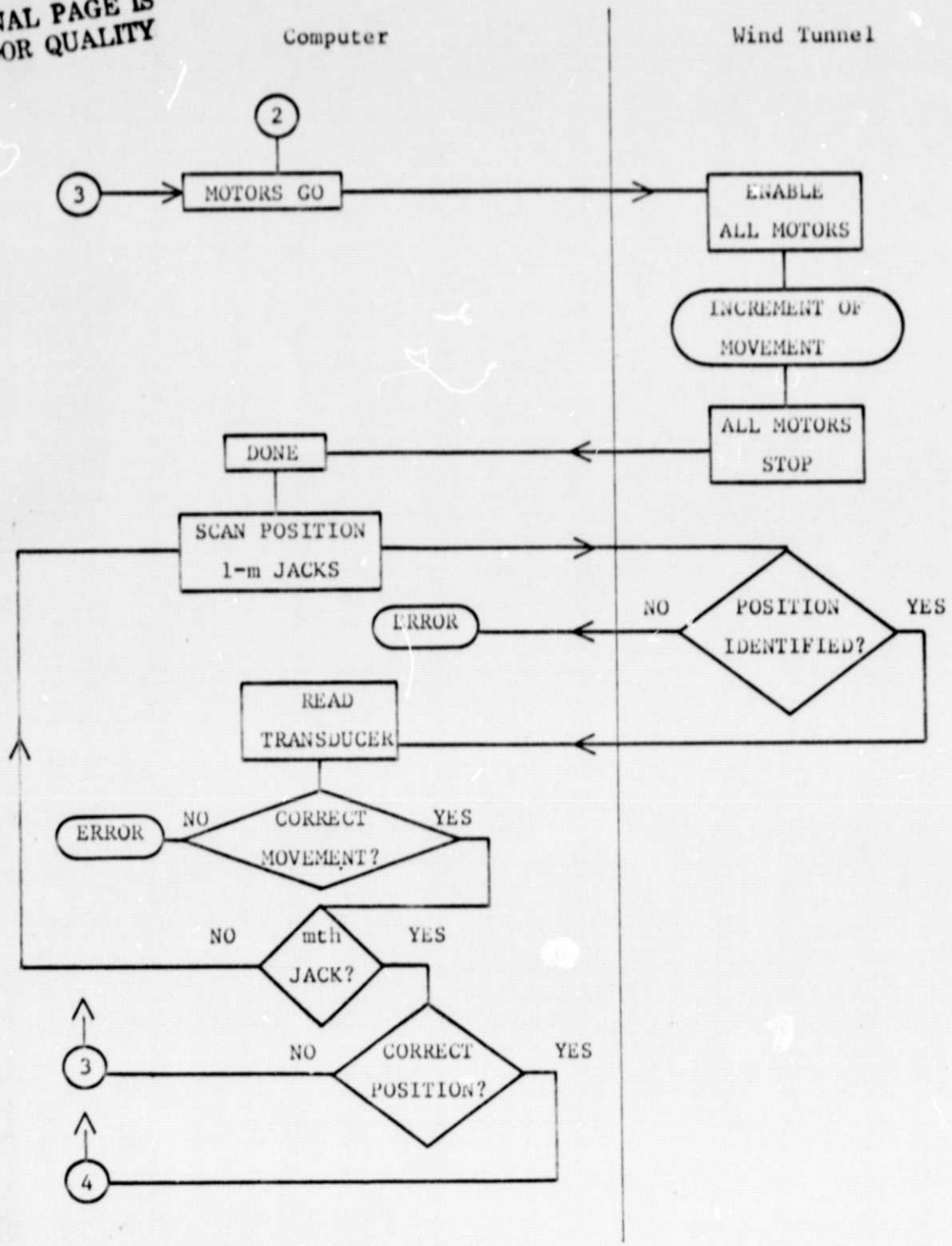


Figure 4.1c CONTROL SYSTEM FLOW DIAGRAM FOR TRANSONIC TEST SECTION (Continued)

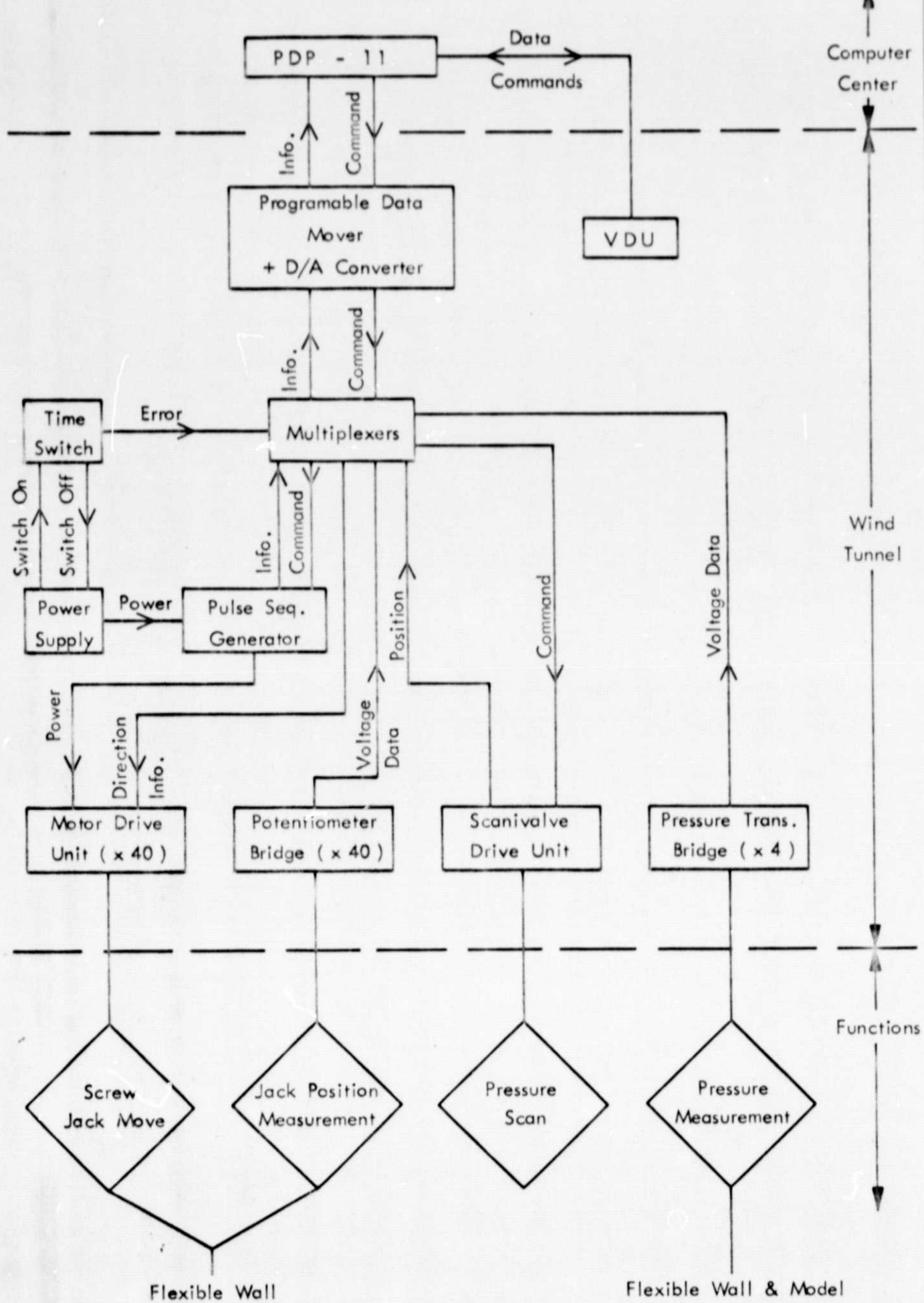
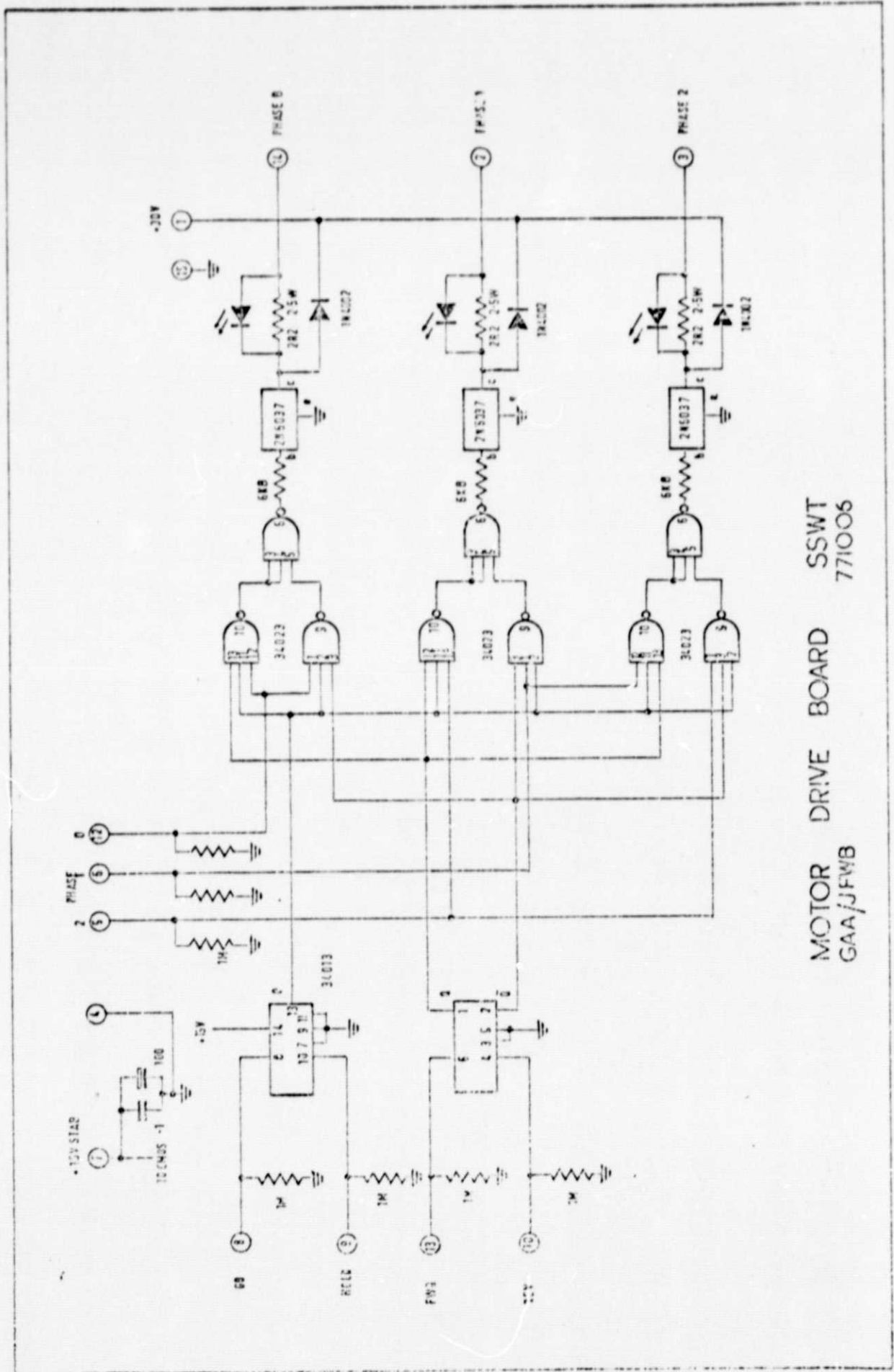


Figure 4.2 TSWT CONTROL SYSTEM HARDWARE.





MOTOR DRIVE BOARD SSWT  
GAA/JFWB 771006

Figure 4.3b CIRCUIT DIAGRAM OF THE MOTOR DRIVE UNIT

